Supporting Information for

Comparative Solution Equilibrium Studies on Anticancer Estradiol-Based Conjugates and Their Copper Complexes

Éva A. Enyedy *, Anett Giricz, Tatsiana V. Petrasheuskaya, János P. Mészáros, Nóra V. May, Gabriella Spengler, Ferenc Kovács, Barnabás Molnár and Éva Frank

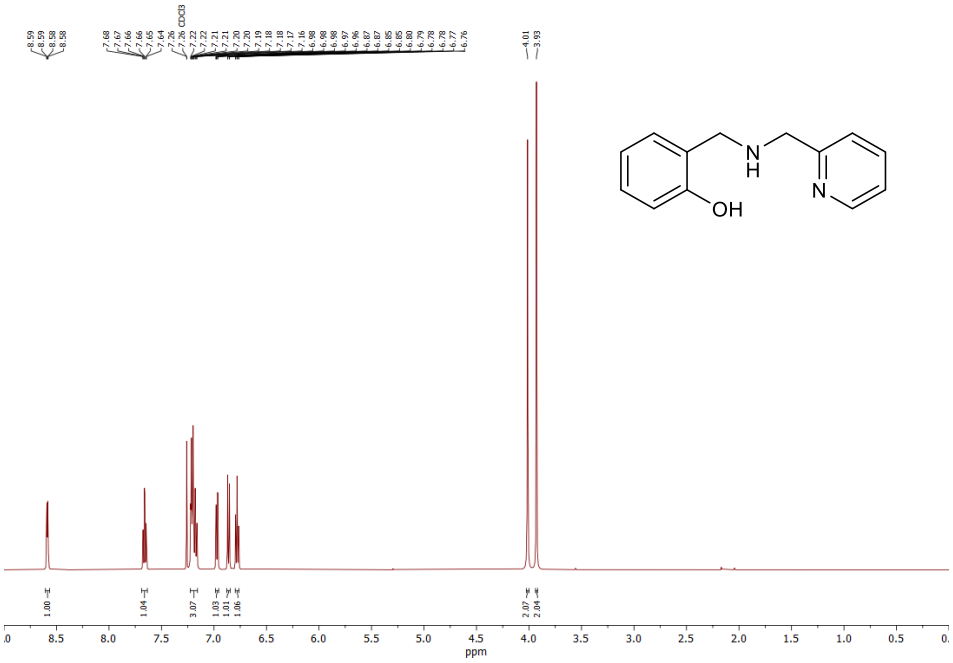

Figure S1. ^{1}H NMR spectrum of PMAP in $CDCl_3$.

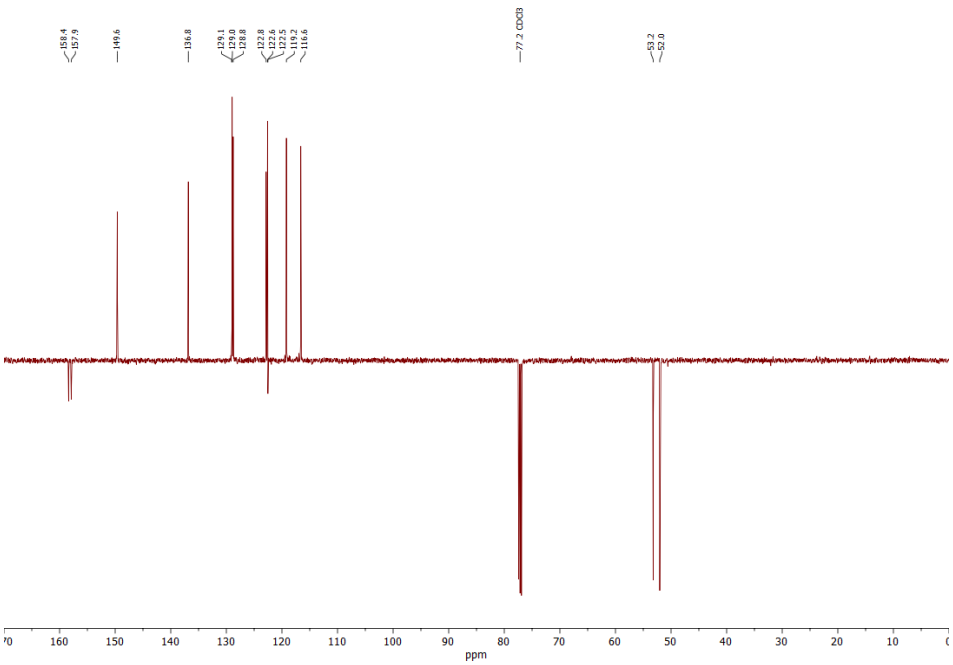

Figure S2. ^{13}C NMR spectrum of PMAP in $CDCl_3$.

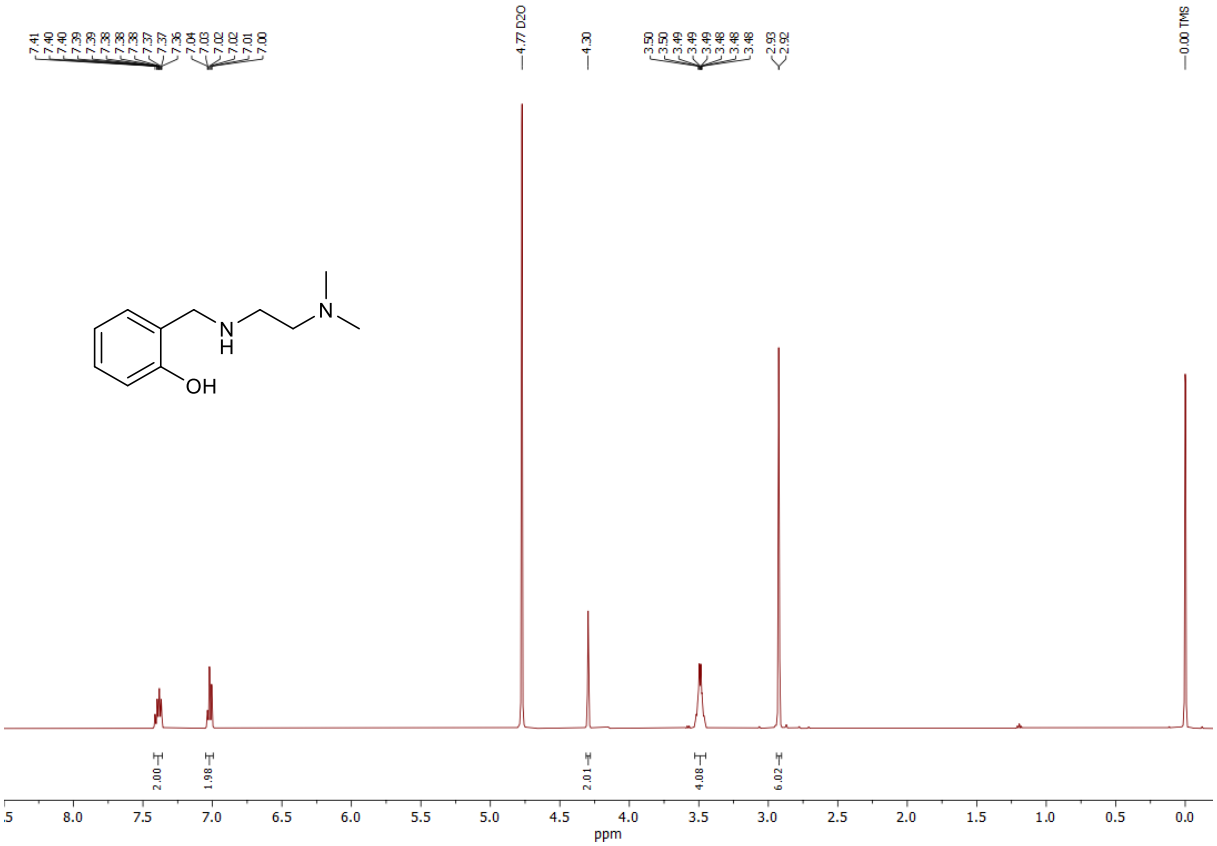

Figure S3. ^{1}H NMR spectrum of DMAP in D_2O.

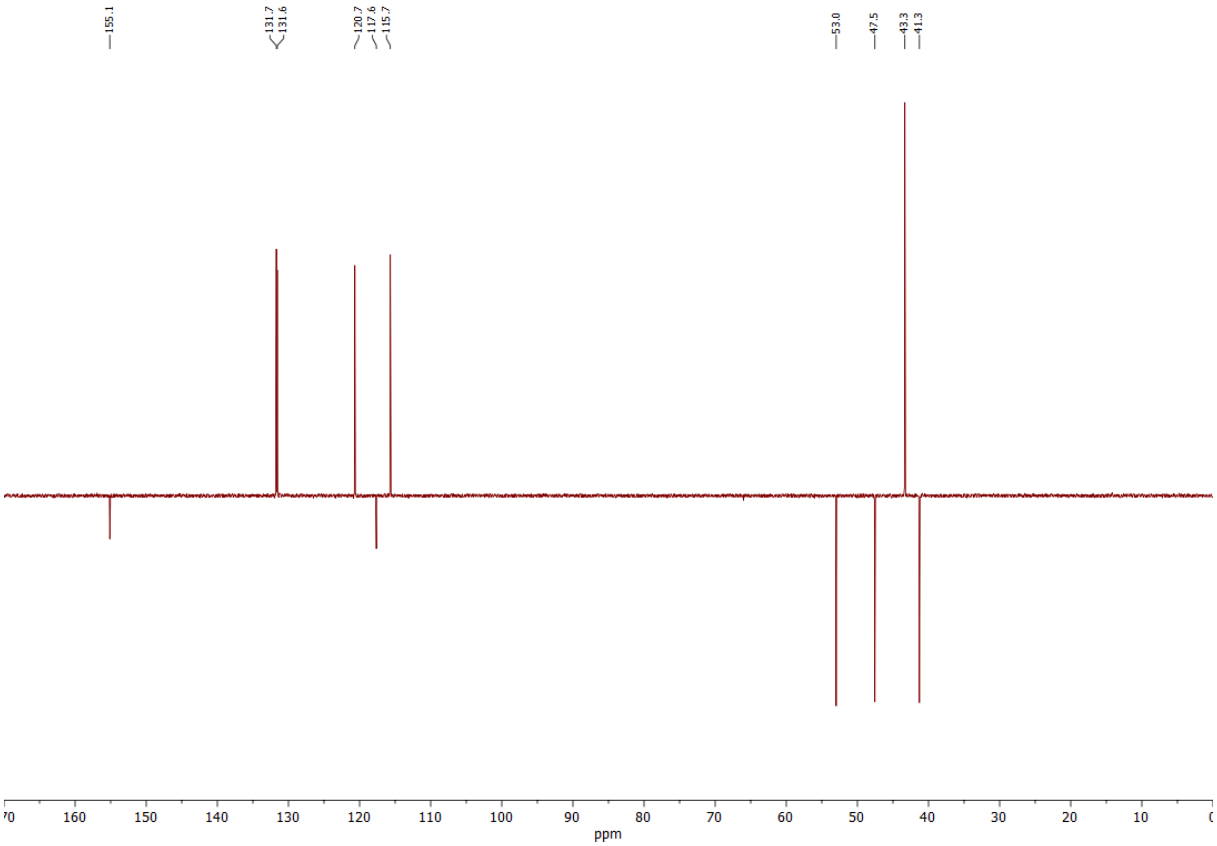

Figure S4. ^{13}C NMR spectrum of DMAP in D_2O.

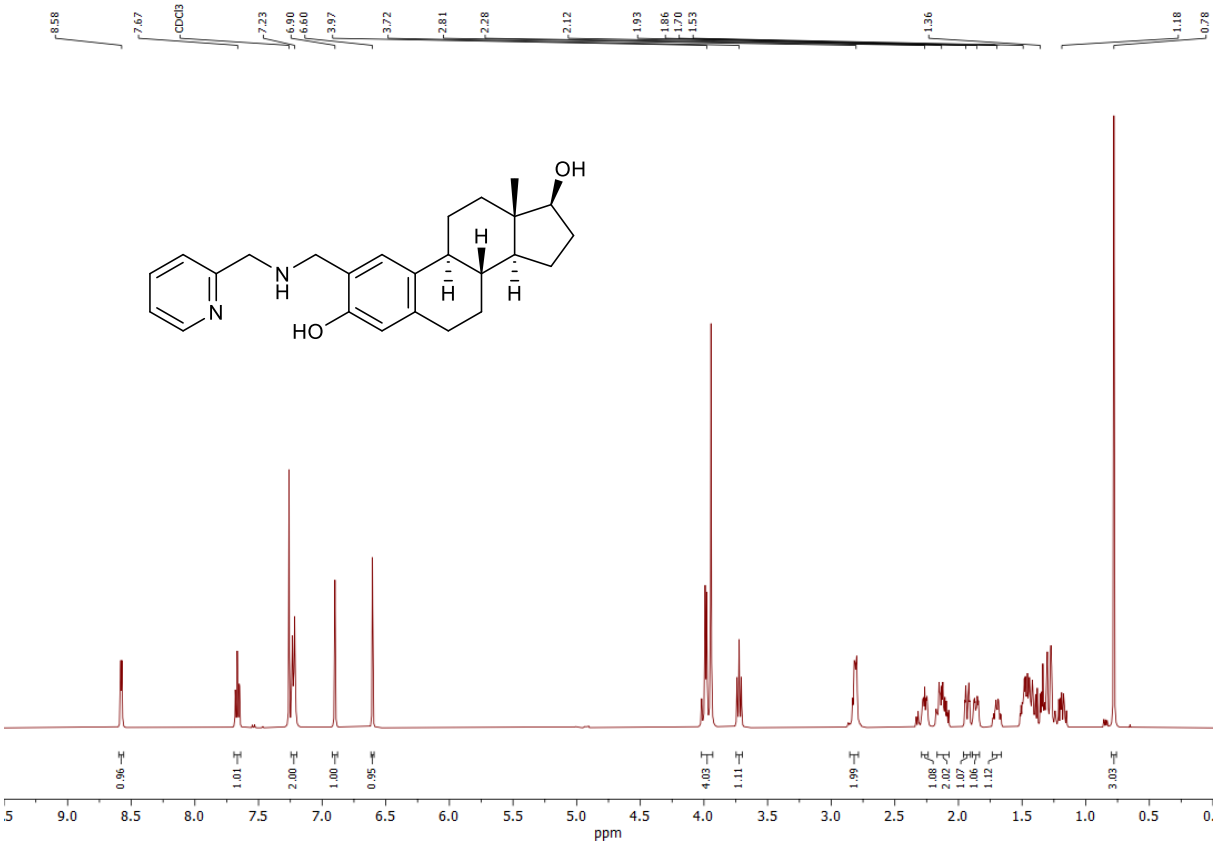

Figure S5. ^{1}H NMR spectrum of PMA-E2 in $CDCl_3$.

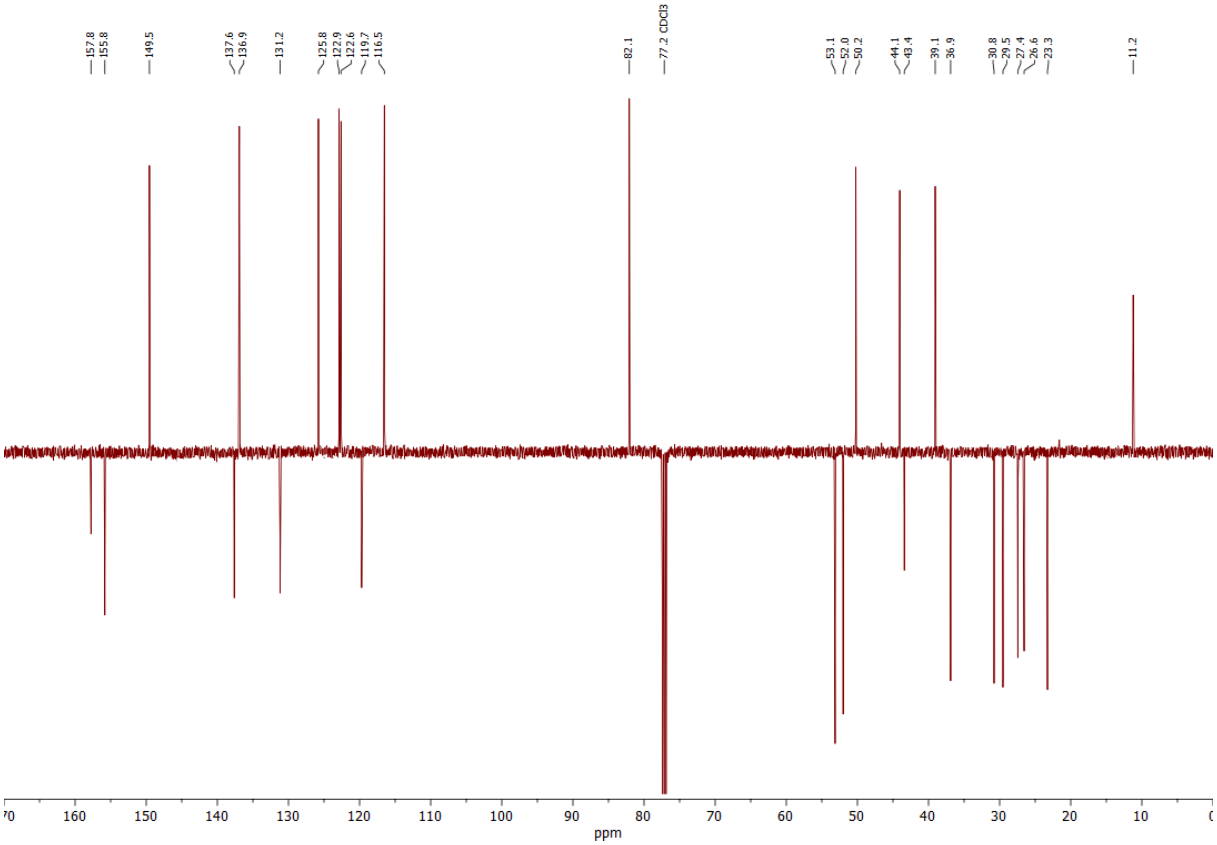

Figure S6. ^{13}C NMR spectrum of PMA-E2 in $CDCl_3$.

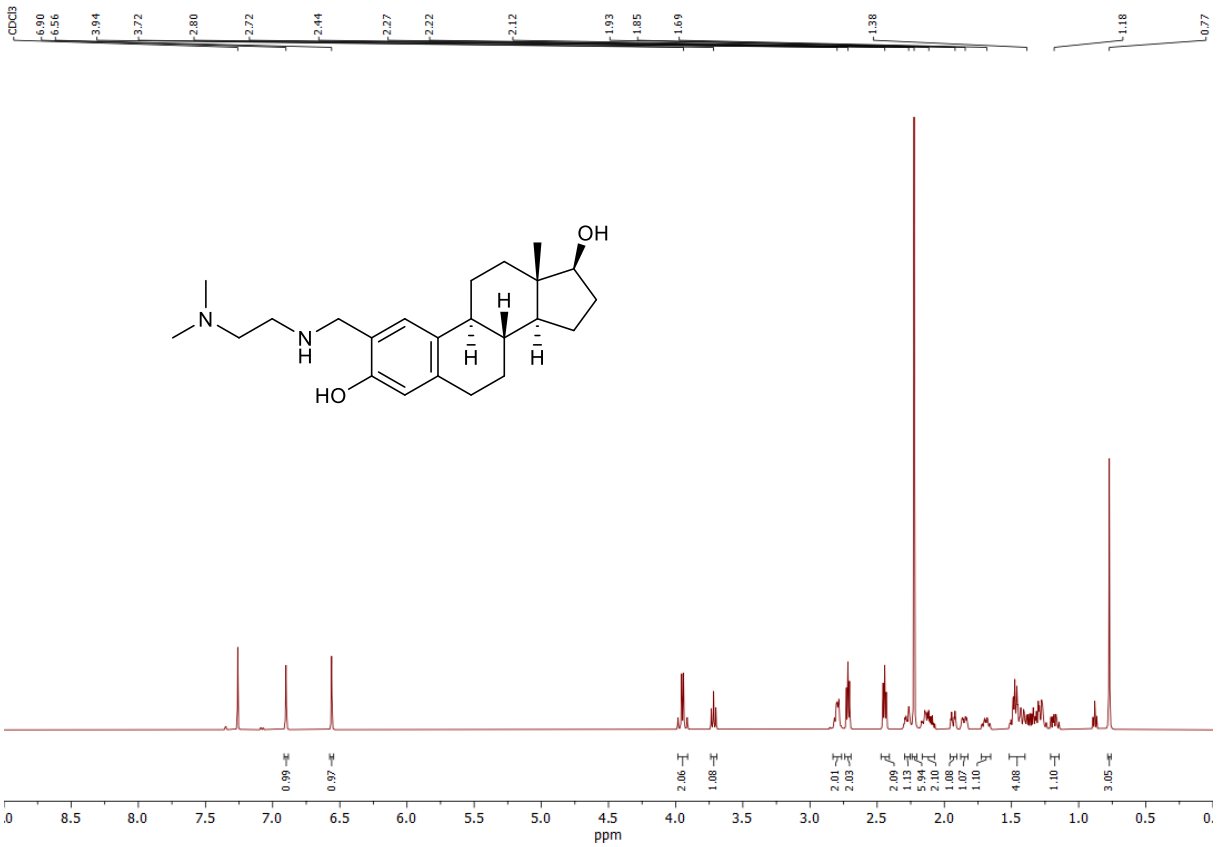

Figure S7. ^{1}H NMR spectrum of DMA-E2 in $CDCl_3$.

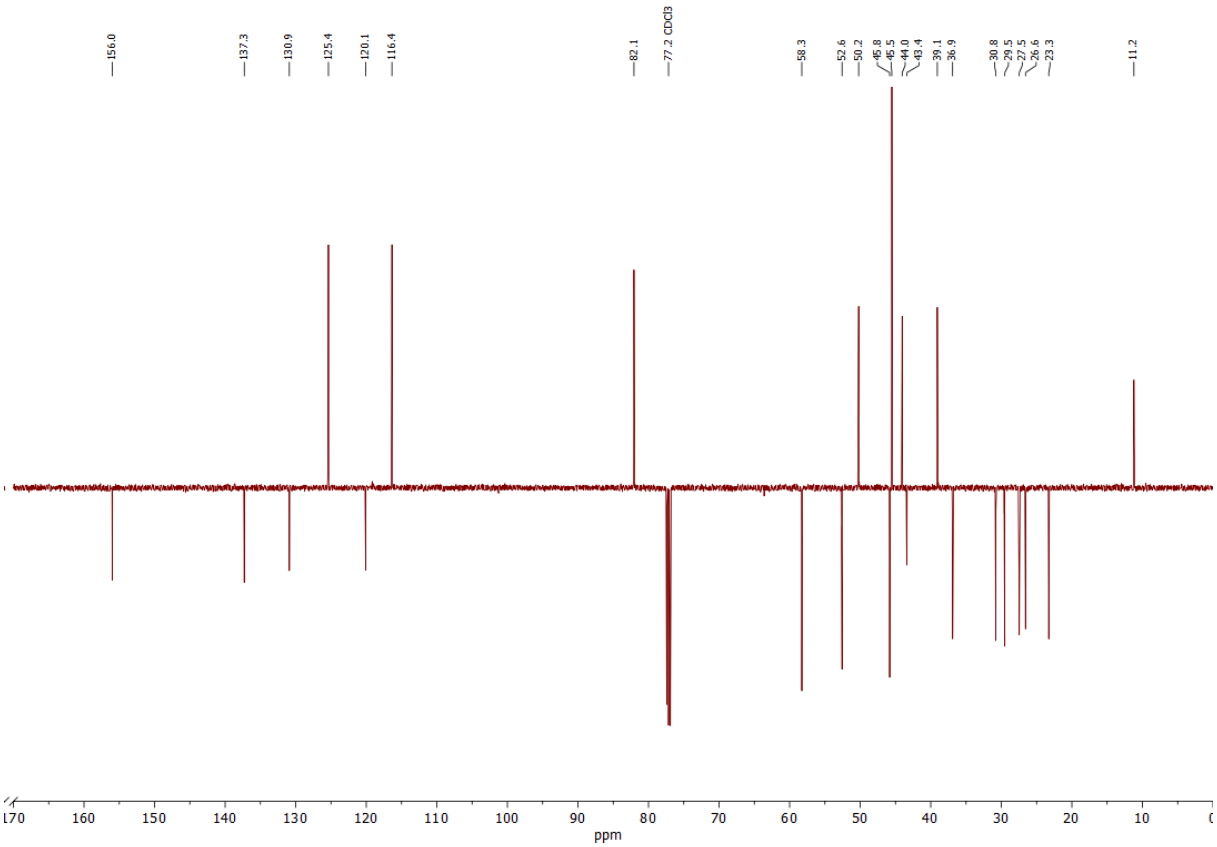

Figure S8. ^{13}C NMR spectrum of DMA-E2 in $CDCl_3$.

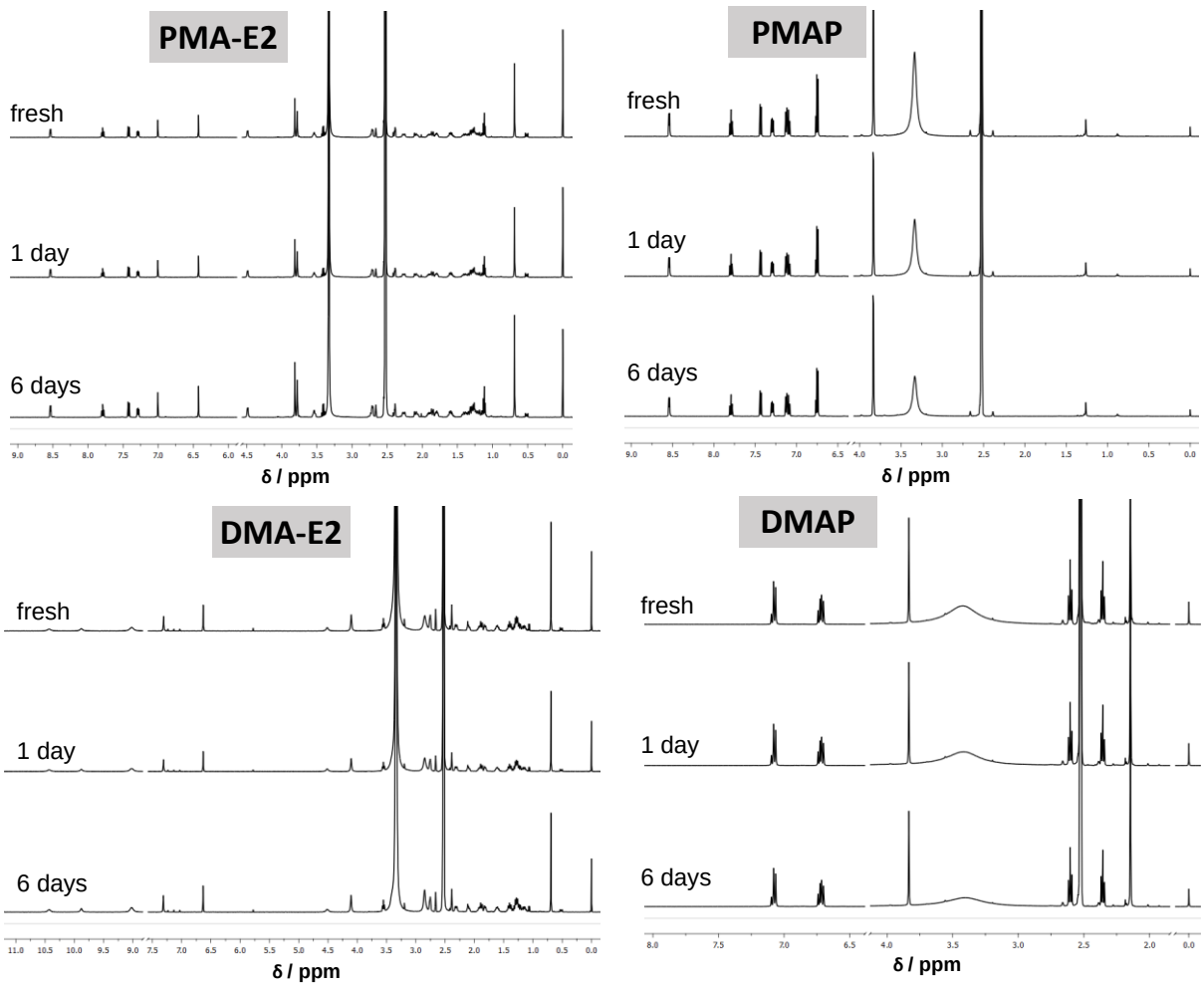

Figure S9. ^{1}H NMR spectra of the studied ligands in d_6-DMSO in their fresh solution and after 1 and 6 days waiting time.

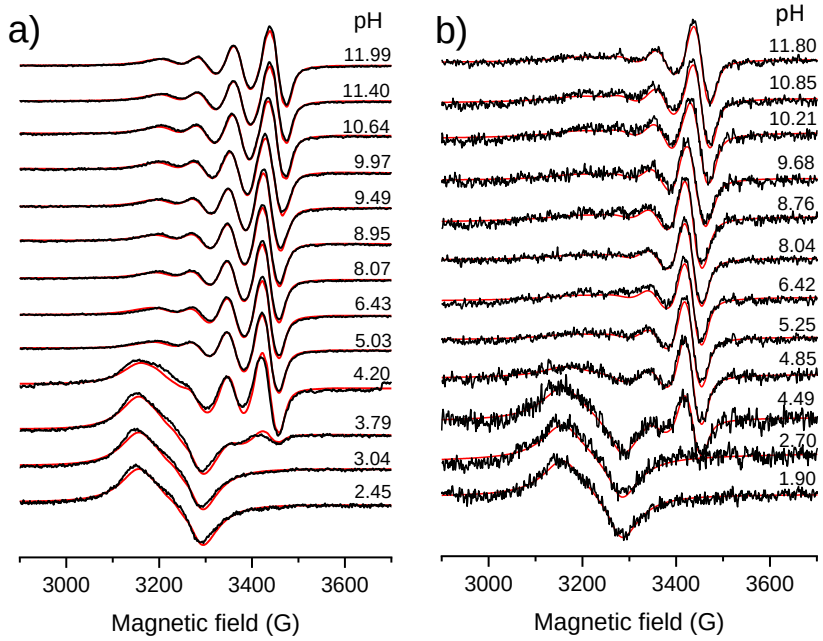

Figure S10. (**a**) pH-dependent experimental (black) and simulated (red) isotropic EPR spectra recorded for the Cu(II) – DMAP system at concentration c_{ligand} = 3.0 mM and $c_{Cu(II)}$ = 2.84 mM, (**b**) and for Cu(II) – DMA-E2 system at concentration c_{ligand} = 0.55 mM and $c_{Cu(II)}$ = 0.43 mM at 295 K. {30% (*v*/*v*) DMSO/H_2O; *I* = 0.10 M (KCl)}

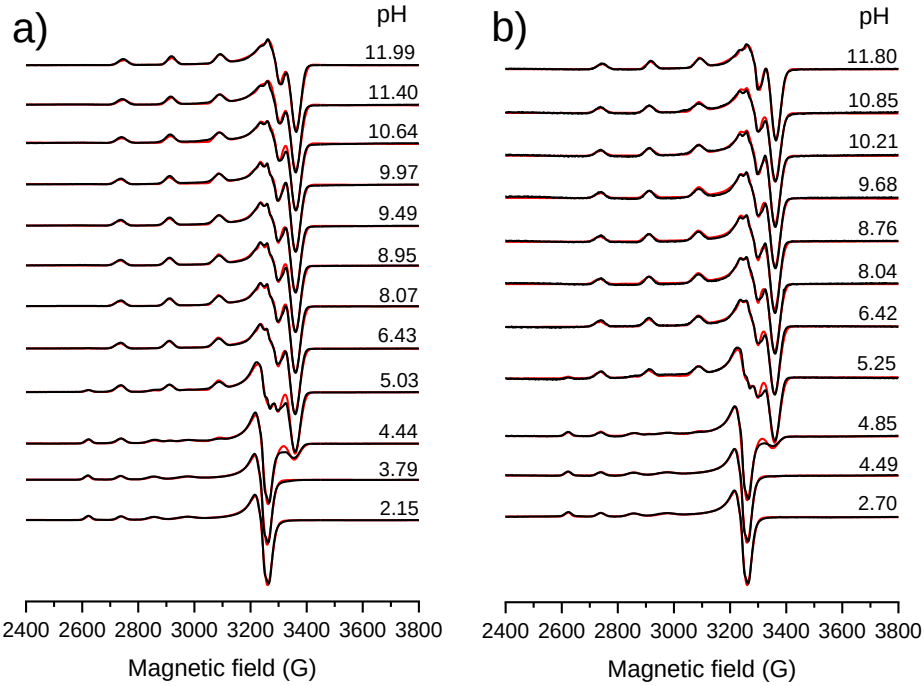

Figure S11. (**a**) pH-dependent experimental (black) and simulated (red) anisotropic EPR spectra recorded for Cu(II) – DMAP system at concentrations of c_{ligand} = 3.0 mM and $c_{Cu(II)}$ = 2.84 mM, (**b**) and for Cu(II) – DMA-E2 system at concentrations of c_{ligand} = 0.55 mM and $c_{Cu(II)}$ = 0.43 mM at 77 K. {30% (*v*/*v*) DMSO/H_2O; *I* = 0.10 M (KCl)}

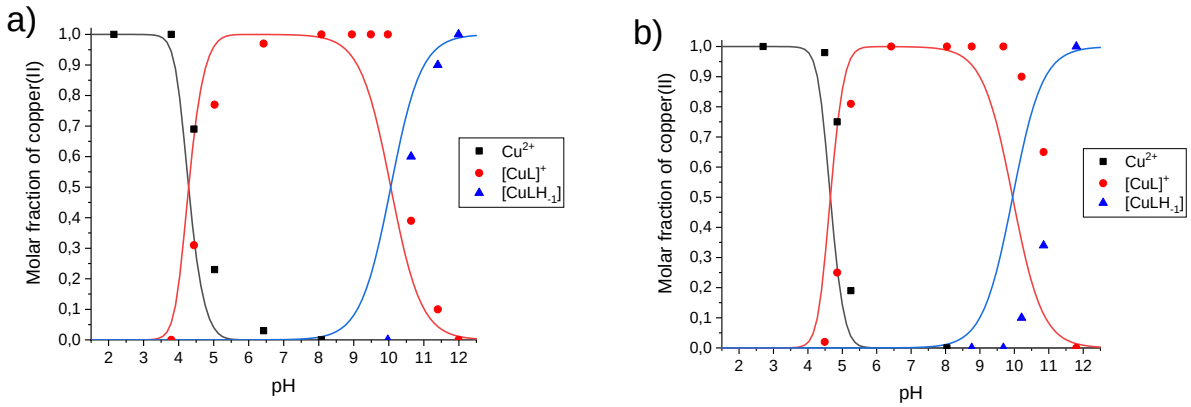

Figure S12. Concentration distribution curves at the concentrations of the EPR measurements using the formation constants obtained by pH-potentiometric (DMAP) or UV-vis spectrophotometric (DMA-E2) titrations (lines) and the component ratios (scatter) obtained by the simulation of frozen solution EPR spectra for (**a**) Cu(II) – DMAP and (**b**) Cu(II) – DMA-E2 systems.

Table S1. Electrochemical data collected for Cu(II) – DMAP, Cu(II) – DMA-E2 and Cu(II) – PMAP systems at pH 7.4 using 10 mV/s scan rate. {30% (*v*/*v*) DMF/H_2O, c_{ligand} = 0.60 or 0.55 mM, $c_{Cu(II)}$ = 0.50 mM; glassy carbon working electrode, Pt auxiliary electrode, Ag/AgCl/KCl (3 M) reference electrode, 0.1 M KNO_3 supporting electrolyte}

	DMAP	**DMA-E2**	**PMAP**
E_c / **mV**	–452	–486	–450
E_a / **mV**	–215	–315	–280
ΔE / **mV**	237	171	178
$E_{1/2}$ / **mV**	–333	–400	–365
$E_{1/2}$ / **mV** *vs.* **NHE**	–123	–190	–155
$\lvert i_c/i_a \rvert$	1.22	1.13	1.00

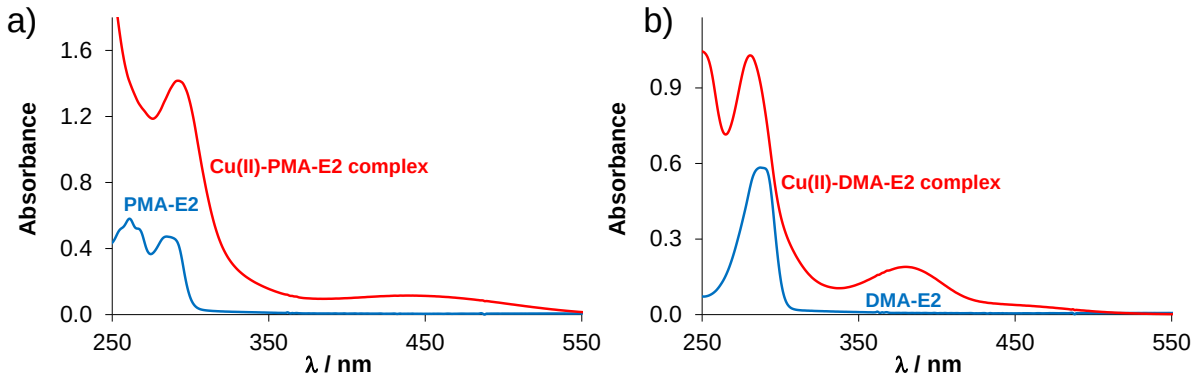

Figure S13. (**a**) UV-vis absorption spectra of PMA-E2 and its Cu(II) complex and (**b**) DMA-E2 and its Cu(II) complex in methanol. {c_{PMA} = 170 μM; $c_{Cu(II)\text{-}PMA}$ = 230 μM; c_{DMA} = 160 μM; $c_{Cu(II)\text{-}DMA}$ = 110 μM; ℓ = 1 cm}

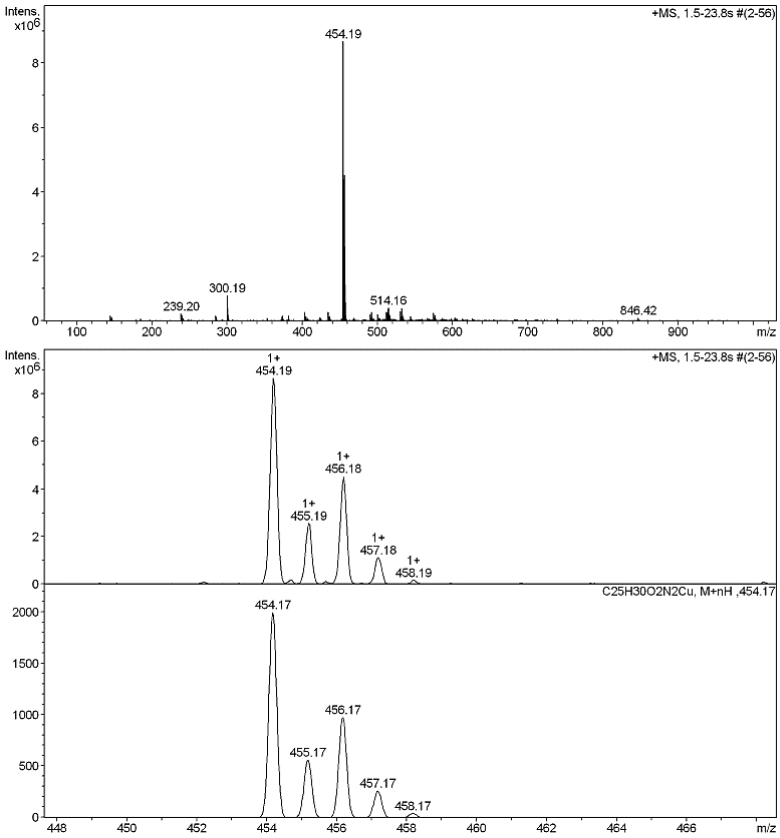

Figure S14. Low-resolution ESI-MS spectra of Cu(II) complex of PMA-E2 [CuLCl]. Sample was prepared in methanol (m/z $[CuL]^+$ found 454.19, calcd. 454.17 for $C_{25}H_{31}N_2O_2Cu$).

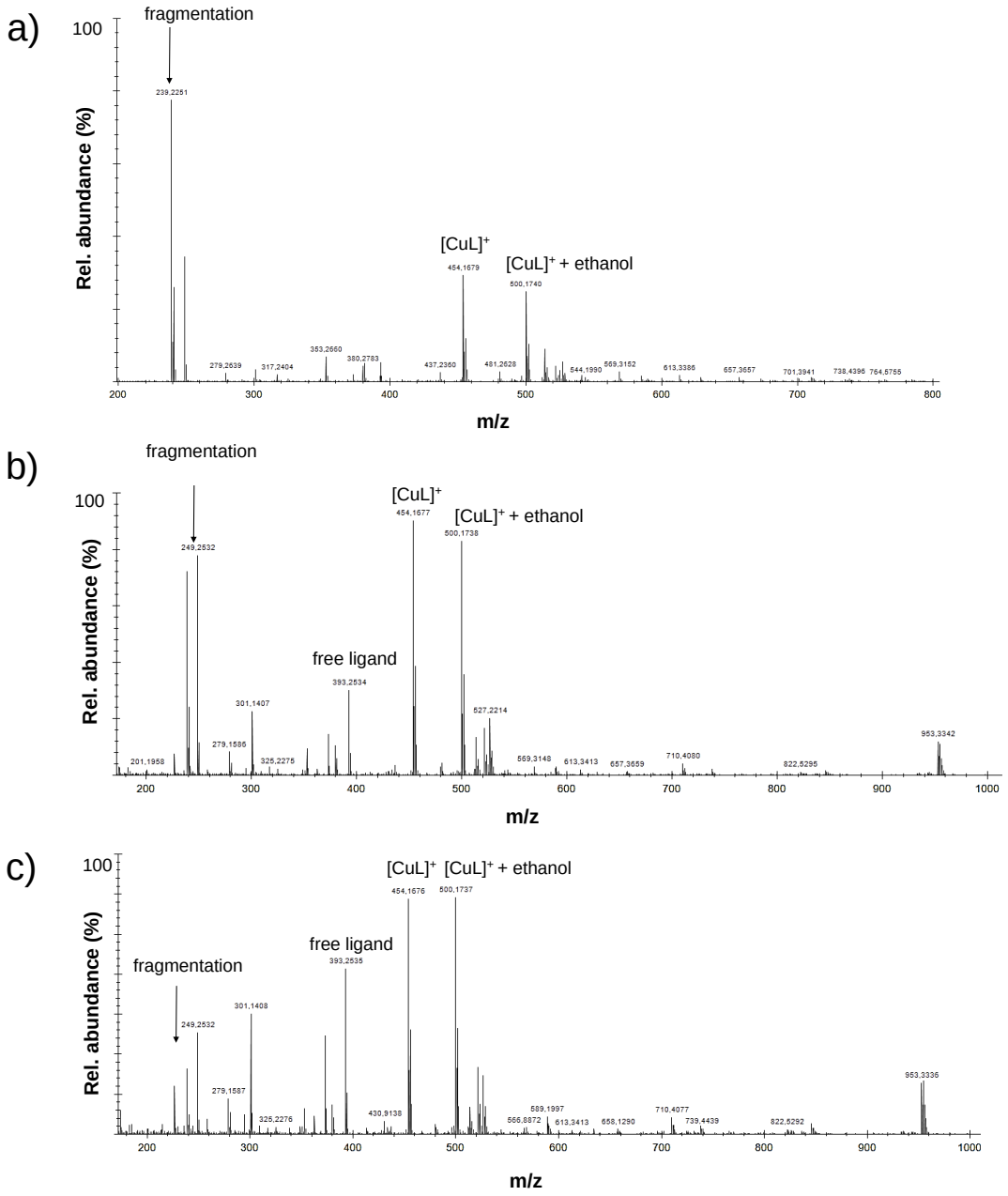

Figure S15. High-resolution ESI-MS spectra of Cu(II) complex of PMA-E2 [CuLCl]. Sample was prepared in methanol. (**a**) Scan time: 0.63 min. (m/z $[CuL]^+$ found 454.1679, calcd. 454.1682 for $C_{25}H_{31}N_2O_2Cu$; $[CuL]^+$ + ethanol found 500.1740, calcd. 500.2100 for $C_{25}H_{31}N_2O_2Cu + C_2H_5OH$). (**b**) Scan time: 0.68 min. (m/z $[CuL]^+$ found 454.1677, calcd. 454.1682 for $C_{25}H_{31}N_2O_2Cu$; $[CuL]^+$ + ethanol found 500.1738, calcd. 500.2100 for $C_{25}H_{31}N_2O_2Cu + C_2H_5OH$). (**c**) Scan time: 0.73 min. (m/z $[CuL]^+$ found 454.1676, calcd. 454.1682 for $C_{25}H_{31}N_2O_2Cu$; $[CuL]^+$ + ethanol found 500.1737, calcd. 500.2100 for $C_{25}H_{31}N_2O_2Cu + C_2H_5OH$).

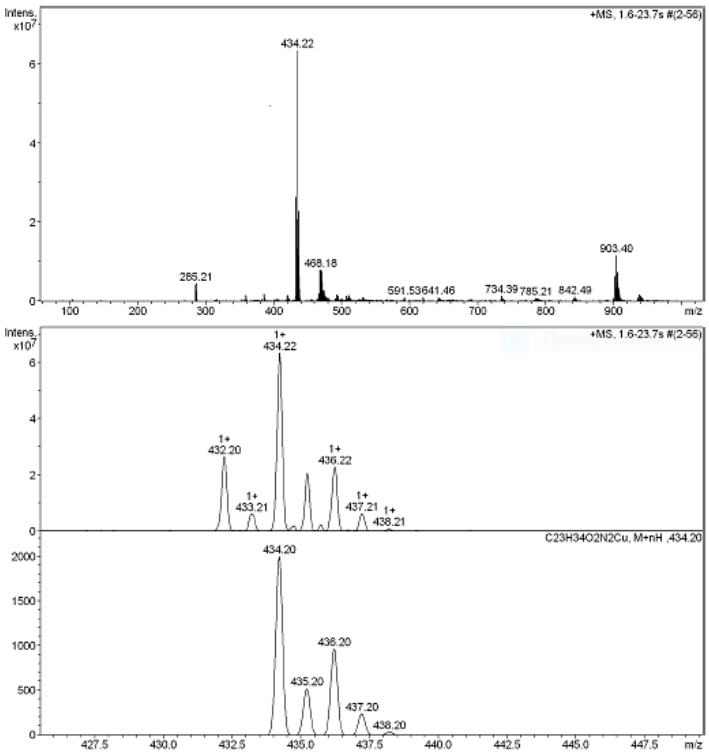

Figure S16. Low-resolution ESI-MS spectra of Cu(II) complex of DMA-E2 [CuLCl]. Sample was prepared in methanol (m/z $[CuL]^+$ found 434.22, calcd. 434.20 for $C_{23}H_{35}N_2O_2Cu$).

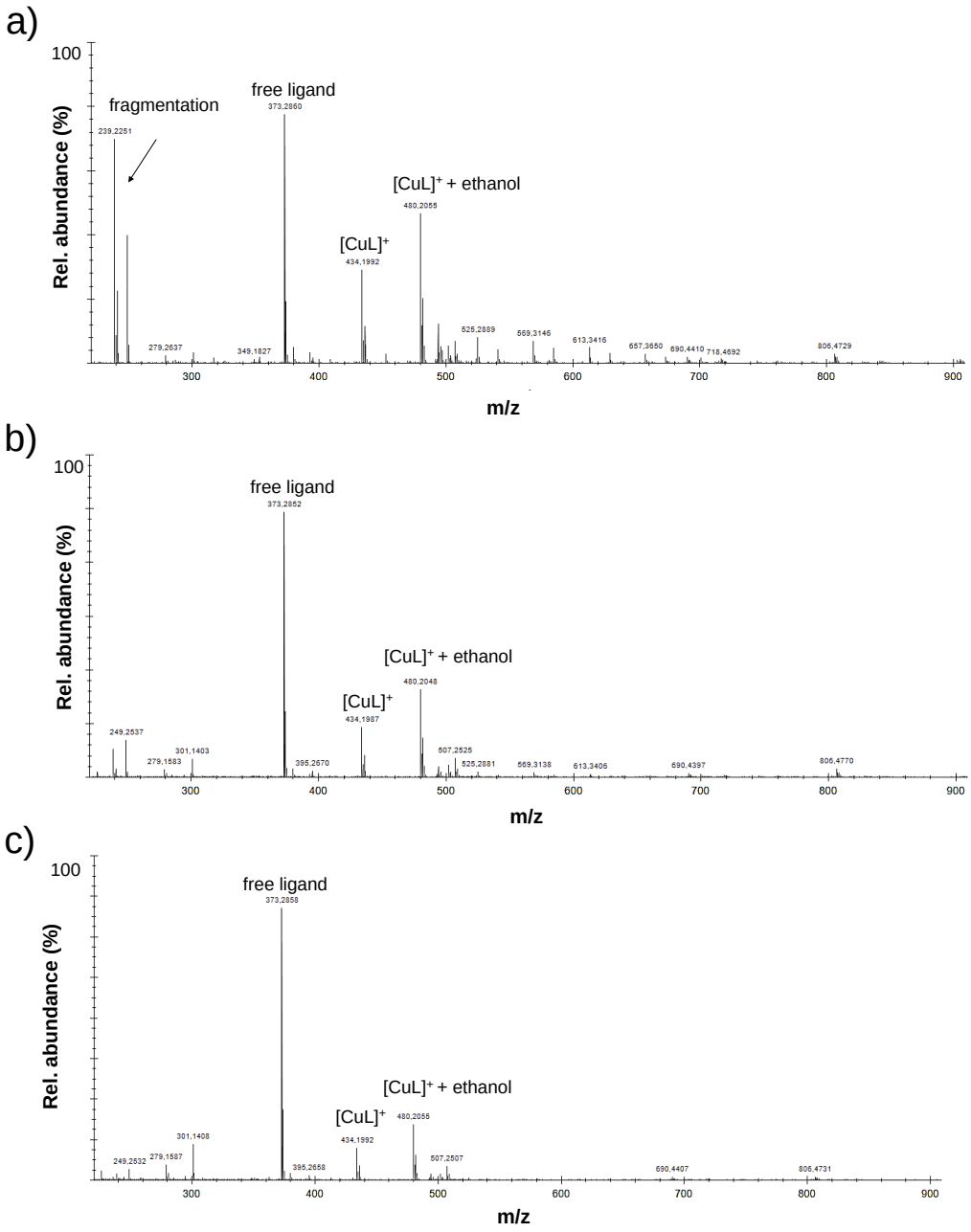

Figure S17. High-resolution ESI-MS spectra of Cu(II) complex of DMA-E2 [CuLCl]. Sample was prepared in methanol. (**a**) Scan time: 0.28 min. (m/z $[CuL]^+$ found 434.1992, calcd. 434.1995 for $C_{23}H_{35}N_2O_2Cu$; $[CuL]^+$ + ethanol found 480.2055, calcd. 480.2413 for $C_{23}H_{35}N_2O_2Cu + C_2H_5OH$). (**b**) Scan time: 0.33 min. (m/z $[CuL]^+$ found 434.1987, calcd. 434.1995 for $C_{23}H_{35}N_2O_2Cu$; $[CuL]^+$ + ethanol found 480.2048, calcd. 480.2413 for $C_{23}H_{35}N_2O_2Cu + C_2H_5OH$). (**c**) Scan time: 0.38 min. (m/z $[CuL]^+$ found 434.1987, calcd. 434.1992 for $C_{23}H_{35}N_2O_2Cu$; $[CuL]^+$ + ethanol found 480.2055, calcd. 480.2413 for $C_{23}H_{35}N_2O_2Cu + C_2H_5OH$).

NOTE: It should be noted that the DMA-E2 complex appeared exclusively in the low-resolution ESI-MS spectrum, whereas the signal of the free ligand was found in the high-resolution spectra (increased signal with increased scan time), which may be due to dissociation of the Cu(II) complex under the condition of the measurement.

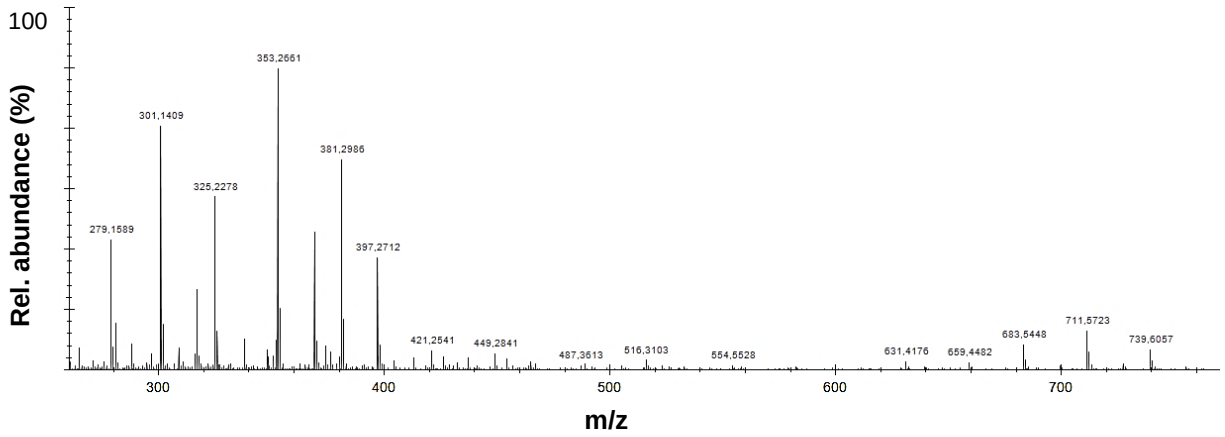

Figure S18. Background spectrum for the high resolution ESI-MS measurements.

Table S2. EPR parameters [a] of the complexes determined at 77 K (anisotropic) from the EPR spectra recorded for the isolated Cu(II) complex of DMA-E2 and PMA-E2, together with the parameters of $[CuL]^+$ and $[CuLH_{-1}]$ complexes of DMAP and reference data for Cu(II) complexes of salicylaldehyde (2-(2-hydroxybenzylidene)hydrazinecarboximidamide (SISC) [1], (E)-2-((3-aminopyridin-2-yl)methylene)hydrazinecarboxamide (oxo-triapine) [2], and the dipeptides F-*c*ACHC [3] and F-*t*ACHC [3] bearing (*N*,*N*,*O*) coordination mode.

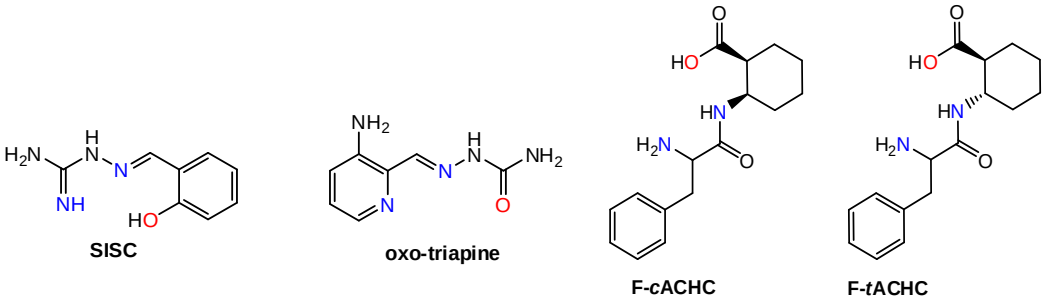

	complex	coordination mode	g_x	g_y	g_z	A_x	A_y	A_z	$g_{0,calcd}$
DMA-E2	isolated	(*N*,*N*,*O*$^-$)	2.055	2.055	2.244	27	27	177	2.118
PMA-E2	isolated	(*N*,*N*,*O*$^-$)	2.051	2.051	2.256	20	20	178	2.119
DMAP	$[CuL]^+$	(*N*,*N*,*O*$^-$)	2.050	2.050	2.248	24	24	181	2.116
	$[CuLH_{-1}]$	(*N*,*N*$^-$,*O*$^-$)	2.047	2.047	2.242	23	23	176	2.112
SISC	$[CuL]^+$	(*N*,*N*,*O*$^-$)	2.034	2.056	2.248	19	22	174	2.113
	$[CuLH_{-1}]$	(*N*,*N*,*O*$^-$)(*OH*$^-$)	2.045	2.048	2.245	14	21	176	2.113
oxo-triapine	$[CuL]^+$	(*N*,*N*,*O*$^-$)	2.054	2.054	2.255	16	16	156	2.121
F-*c*ACHC	$[CuLH_{-1}]$	(*N*,*N*,*O*$^-$)	2.038	2.053	2.237	23	19	191	2.109
F-*t*ACHC	$[CuLH_{-1}]$	(*N*,*N*,*O*$^-$)	2.040	2.057	2.252	18	21	182	2.116

[a] The coupling values are given in 10^{-4} cm^{-1}, the relaxation parameters are in G. The experimental error was ±0.001 for g and ±1 × 10^{-4} cm^{-1} for A parameters. [b] Calculated by the equation $g_0 = (g_x + g_y + g_z)/3$.

References

1. Dömötör, O.; May, N.V.; Gál, G.T.; Spengler, G.; Dobrova, A.; Arion, V.B.; Enyedy, É.A. Solution Equilibrium Studies on Salicylidene Aminoguanidine Schiff Base Metal Complexes: Impact of the Hybridization with L-Proline on Stability, Redox Activity and Cytotoxicity. *Molecules* **2022**, *27*, 2044.
2. Enyedy, É.A.; May, N.V.; Pape, V.F.S.; Heffeter, P.; Szakács, G.; Keppler, B.K., Kowol, C.R. Complex formation and cytotoxicity of Triapine derivatives: A comparative solution study on the effect of the chalcogen atom and NH-methylation. *Dalton Trans.* **2020**, *49*, 16887–16902.
3. Nagy, N.V.; Doorslaer, S.V.; Szabó-Plánka, T.; Rompaey, S.V.; Hamza, A.; Fülöp, F.; Tóth, G.K.; Rockenbauer, A. Copper (II)-binding ability of stereoisomeric *cis*-and *trans*-2-aminocyclohexanecarboxylic acid–l-phenylalanine dipeptides. A combined cw/pulsed EPR and DFT study. *Inorg. Chem.* **2012**, *51*, 1386–1399.